KOH-activated porous carbon from *Mucuna monosperma* seeds for supercapacitor applications

Sabina Sapkota*, Pushpa Regmi*, Nanda Bikram Adhikari and Mandira Pradhananga Adhikari***

*Central Department of Chemistry, Tribhuvan University; 44613 Kirtipur, Kathmandu, Nepal.

**Department of Electronics and Computer Engineering, Pulchowk Campus, 44600, Pulchowk, Lalitpur.

Abstract: Biomass-derived activated carbon has emerged as a promising low-cost and sustainable electrode material for electrochemical energy storage applications. In this work, activated carbon was synthesized from *Mucuna monosperma* seed biomass via chemical activation with potassium hydroxide (KOH), followed by carbonization and activation at 700 °C to develop a porous carbon structure (BSC_700). Physicochemical characterization using iodine number, methylene blue adsorption, Boehm titration, Fourier transform infrared spectroscopy (FTIR), and X-ray diffraction (XRD) confirmed the formation of predominantly amorphous carbon with well-developed porosity and surface functional groups, with a specific surface area of 1360 m^2 g^{-1} estimated by using the multi-point methylene blue adsorption technique. The electrochemical performance of the prepared activated carbon was evaluated in a three-electrode configuration using cyclic voltammetry, galvanostatic charge-discharge, and electrochemical impedance spectroscopy with 6 M KOH as the electrolyte. The electrode exhibited electrical double-layer capacitive behavior and delivered a good specific capacitance of 333.8 Fg^{-1} at 1 Ag^{-1}, demonstrating good electrochemical reversibility and low internal resistance. These results indicate that *Mucuna monosperma* seed- derived activated carbon is an efficient, environmentally friendly, and promising electrode material for supercapacitor applications.

Keywords: Activated carbon; Chemical activation; Cyclic voltammetry; Methylene blue; Specific capacitance.

Introduction

The growing worldwide demand for efficient and sustainable energy storage systems has spurred research into advanced electrochemical energy storage devices[1,2]. Among these, supercapacitors have attracted considerable attention due to their high-power density, rapid charge-discharge capability, long cycle life, and operational safety[3]. However, the energy density of supercapacitors remains lower than that of conventional batteries, which limits their broader application. The performance of supercapacitors is strongly governed by the nature of the electrode materials, making the development of low-cost, high-performance, and environmentally friendly electrode materials a critical Research focus[4,5,6].

Carbon- based materials are widely used as supercapacitor electrodes because of their excellent electrical conductivity, chemical stability, and highly porous structure[7,8]. Activated carbon, in particular, remains the most commercially suitable electrode material because of its large specific surface area, well-developed porosity, and relatively low production cost[9],[10,11]. In recent years, biomass-derived activated carbon has gained significant interest as a sustainable alternative to conventional fossil-based carbon precursors. Agricultural residues, fruit shells, seeds, and other biomass wastes are abundant, renewable, and inexpensive, making them attractive raw materials for carbon production[12,13].

Moreover, the internal composition and structure of biomass can facilitate the development of porous structures

Author for correspondence: Mandira Pradhananga Adhikari, Central Department of Chemistry, Tribhuvan University, Kathmandu, Nepal.
Email: mandira43@hotmail.com: adhikari@ioe.edu.np; https://orcid.org/0000-0002-5183-8343
Received: 9 Feb, 2026; Received in revised form: 4 Apr, 2026; Accepted: 10 Apr, 2026.
Doi: https://doi.org/10.3126/sw.v19i19.95673

during carbonization and chemical activation. Chemical activation using potassium hydroxide (KOH) is particularly effective in producing highly porous carbon materials with enhanced surface area and improved electrochemical properties, even at relatively moderate activation temperatures[14,15]. Seed-based biomass precursors have been reported to yield activated carbons with favorable micro and mesoporous structures suitable for supercapacitor applications[16]. Nevertheless, many naturally available seed biomasses remain unexplored, especially those that are locally abundant and underutilized. *Mucuna monosperma*, a leguminous plant widely found in Nepal and neighboring regions, produces seeds that are rich in carbonaceous content and are generally considered non- edible biomass. Despite this potential, there are limited reports on the utilization of *Mucuna monosperma* seeds as a precursor for activated carbon, particularly for electrochemical energy storage applications.

In this context, the present work aims to synthesize activated carbon from the seed of *Mucuna monosperma* (locally known as Baldhyangra). Hereafter, it is referred to as BSP. Chemical activation was done using KOH. The prepared activated carbon was systematically characterized to investigate its thermal behavior, surface chemistry, and structural properties. Furthermore, the electrochemical performance of the material was evaluated using cyclic voltammetry, galvanostatic charge-discharge, and electrochemical impedance spectroscopy in an alkaline electrolyte. This study highlights the potential of *Mucuna monosperma* seeds as a low-cost and sustainable precursor for the development of activated carbon electrodes for energy storage applications.

Materials and Methods

Materials

Mucuna monosperma seeds were collected locally and used as the biomass precursor for the preparation of activated carbon. Potassium hydroxide (KOH, analytical grade) was employed as the chemical activating agent. All other chemicals used in the study were of analytical grade and used without further purification. Deionized water was used throughout the experimental procedures.

Preparation and characterization of activated carbon

The collected *Mucuna monosperma* seeds were washed thoroughly with deionized water to remove surface impurities, followed by drying at 80 °C for 6 hours. To investigate the effect of chemical activation, two types of samples were prepared. For the activated sample, dried seeds were crushed and pre-carbonized in an oven at 250 °C for 3 hours to obtain the pre- carbonized precursor. Chemical activation was carried out by impregnating the pre- carbonized material with KOH at a weight ratio of 1:10 (carbon: KOH) and left for 24 hours. The mixture was dried to remove excessive moisture and subsequently carbonized at 700 °C for 3hours in a split-tube furnace in an inert environment maintained by the flow of nitrogen gas at a flow rate of 140 mL min^{-1}. After activation, the product was repeatedly washed with 0.1 M hydrochloric acid and deionized water until neutral pH was achieved, followed by drying to obtain the final activated carbon sample (BSC_700), which was then again crushed and sieved using a sieve of size 185µm. For comparison, a directly carbonized sample (BSC_DC_700) was also prepared under identical conditions without the use of any activating agent. In this case, the pre-carbonized precursor was directly carbonized at 700°C for 3 hours under the same nitrogen atmosphere, followed by similar washing and drying procedures. Proximate analysis of the raw precursor was performed to determine moisture content, volatile matter, ash content, and fixed carbon. Thermogravimetric analysis (TGA) and Derivative Thermogravimetric analysis (DTGA) were carried out to evaluate the thermal stability and decomposition behavior of the biomass precursor.

The porosity characteristics of raw precursor (Raw BSP), directly carbonized at 700ºC (BSC_DC_700), and chemically (KOH) activated carbon (BSC_700) were examined using iodine number and methylene blue adsorption tests. Surface charge behavior of the Activated carbon was evaluated through the point of zero charge (*pHpzc)* analysis. The presence of various oxygen-containing functional groups was revealed by Boehm titration values[17]. Fourier transform infrared (FTIR) spectroscopy (NICOLET iS20, Thermo-Fisher Scientific, Waltham, MA, USA), JASCO, Tokyo, was employed to

identify surface functional groups present on the activated carbon, while X-ray diffraction (XRD) analysis was used to examine the structural and crystallographic features of the prepared carbon.

Electrode preparation and electrochemical measurements

The working electrode was prepared by mixing the activated carbon with a conductive additive, carbon black, and binder, PVDF, in a weight ratio of 8:1:1 using 1 mL of N-Methyl-2-Pyrrolidone (NMP) to form a homogeneous slurry. The slurry was coated onto a nickel foam (1 cm x 1 cm) and dried for about 10 hours in an oven at 60 °C before electrochemical analysis. Electrochemical performance was evaluated in a three-electrode configuration using the prepared electrode as the working electrode, a platinum wire as the counter electrode, and an external reference electrode. Aqueous 6 M KOH solution was used as the electrolyte. Cyclic voltammetry (CV), Galvanostatic charge-discharge (GCD), and Electrochemical impedance spectroscopy (EIS) measurements were carried out to assess the capacitive behavior, charge-discharge characteristics, and internal resistance of the electrode material. All the measurements were done on a CH Instruments model 660E workstation (CH Instruments, Inc., USA). CV curve was obtained as scan rates ranged from 5 to 200 mV/s, and the potential window was set between -0.1 and 0.6 V. A GCD curve of BSC_700 was obtained at variable current densities of 1 A/g to 5 A/g in 6 M KOH electrolyte.

Specific capacitance of the three-electrode system was calculated from the GCD curve using the formula:

$$C_s = \frac{I\Delta t}{m\Delta v}$$

Where Cs is the specific capacitance (F/g), I is the discharge current (A), Δt is the discharge time (s), m represents the mass of active material in the electrode (g), and ΔV is the change in potential (V).

Results and Discussion

Physicochemical characterization of Activated Carbon

The suitability of *Mucuna monosperma* seed biomass as a carbon precursor was evaluated through proximate analysis and thermogravimetric analysis (TGA). The proximate analysis indicated favorable fixed carbon content (53.7%) with relatively low ash content (2.0%), suggesting its potential for activated carbon production. The TGA profile revealed four stages of weight loss corresponding to moisture removal (100°C), decomposition of hemicellulosic (200°C) & cellulosic components (350°C), and gradual degradation of lignin (500°C).

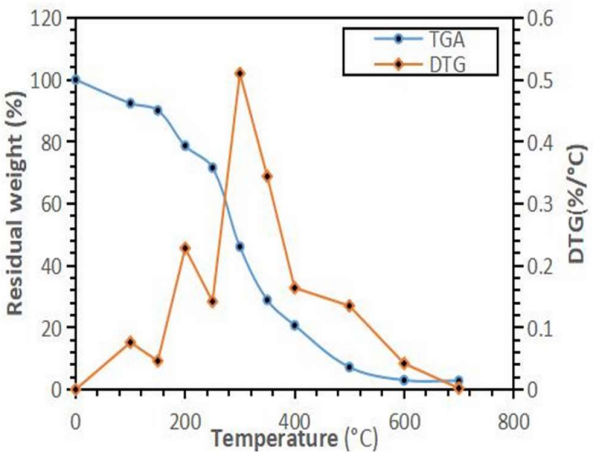

Figure 1: TG and DTG analysis of BSP.

The major weight loss occurred at around 350 °C, which is consistent with the thermal degradation of cellulosic components. In addition, the derivative thermogravimetric (DTG) curve shows distinct peaks corresponding to the maximum rate of weight loss at different stages of decomposition. A prominent DTG peak around ~350 °C is attributed to the rapid degradation of cellulose, while a broader peak at higher temperatures (~400–500 °C) corresponds to the gradual decomposition of lignin. The observed thermal stability at higher temperatures supports the selection of the activation temperature used for carbon preparation. The porosity of the activated carbon was evaluated using iodine number and methylene blue adsorption tests, which are commonly used indicators of micro- and mesoporous structures, respectively.

The activated carbon exhibited an iodine number of 803.7±35.43 and a methylene blue adsorption capacity of674.69±0.76, indicating the development of a well-connected pore network during KOH activation. Such pore characteristics are highly desirable for electrolyte ion diffusion and charge storage in supercapacitor applications

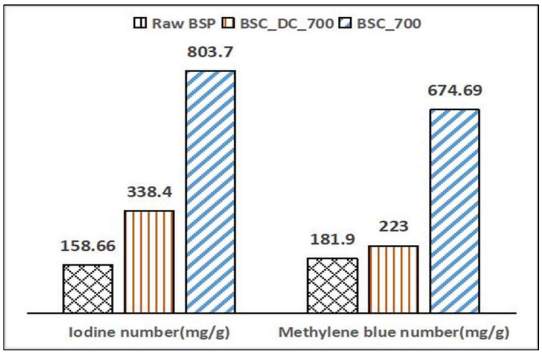

Figure 2: Iodine number and methylene blue absorption of BSP, BSC_DC_700 & BSC_700.

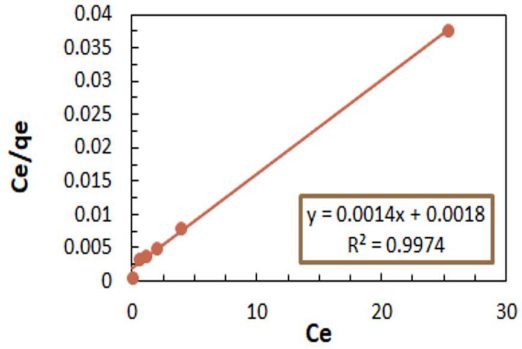

Figure 3: Langmuir model of adsorption isotherm of methylene blue for BSC_700.

The specific surface area of the adsorbent was estimated using the Langmuir isotherm, which assumes monolayer adsorption of adsorbate molecules onto a homogeneous surface with identical active sites. Based on the maximum adsorption capacity (q_{max}=555.56 mg/g) obtained from the Langmuir model, and considering the molecular cross-sectional area of Methylene Blue, the calculated specific surface area was approximately 1360 m^2/g. This relatively high value suggests that the adsorbent possesses a well-developed porous structure and a large number of accessible adsorption sites, contributing to its strong adsorption performance. Furthermore, the excellent fit of the Langmuir model (R^2=0.9974) supports monolayer coverage.

The structural properties of the activated carbon were examined by FTIR and XRD analyses. The FTIR spectrum of raw BSP displayed characteristic absorption bands corresponding to surface functional groups such as hydroxyl, carbonyl, aromatic C=C bonds, C≡C or C≡N stretching of ether and alcohol groups, asymmetric and

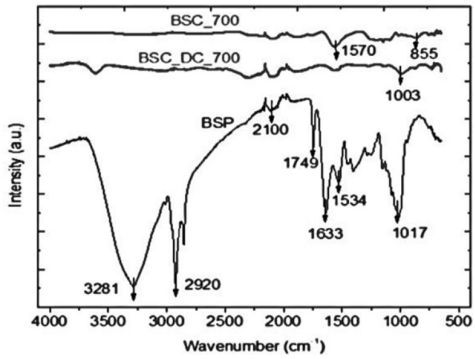

Figure 4: FTIR plot of BSP, BSC_DC_700 & BSC_700.

symmetric C-H stretching of aliphatic -CH_2 and -CH_3 groups, and N-H bending of amide groups, which reflects the oxygen-rich, functionalized nature of raw biomass. After carbonization at 700 °C, a drastic reduction in the number and intensity of absorption bands indicates extensive thermal decomposition and devolatilization of organic functional groups, leading to the formation of a carbon-rich structure.

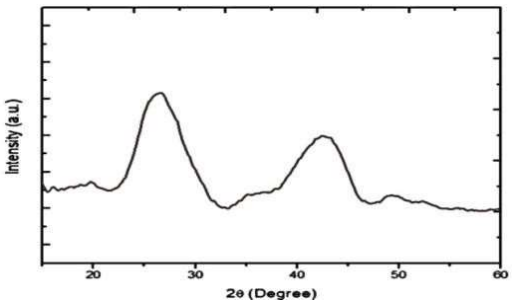

Figure 5: XRD plot of BSC_700.

The XRD pattern exhibited two broad diffraction peaks centered around 2θ ≈ 26°and 2θ ≈ 43°, confirming the predominantly amorphous nature of the carbon material. The absence of sharp crystalline peaks suggests a disordered carbon framework. Surface chemical analysis was done using point of zero charge analysis and Boehm titration. The point of zero charge (*pHpzc*) of the precursor was found to be approximately 7.0, indicating a neutral surface charge at a neutral pH. At alkaline conditions, the surface becomes negatively charged, which is favorable for electrolyte ion interaction in alkaline supercapacitor systems. Boehm titration shows the presence of lactonic (0.35mmole/g), carboxylic (2.7mmole/g), phenolic (0.6), and 0.15 mmole of basic groups, where high acidic group content of 3.65 mmole/g implies suitability for adsorption

of basic groups.

Electrochemical performance of the activated carbon electrode

The electrochemical behavior of the prepared activated carbon was evaluated using cyclic voltammetry (CV), galvanostatic charge-discharge (GCD), and electrochemical impedance spectroscopy (EIS) in a three-electrode configuration with 6 M KOH as the electrolyte. The CV curves exhibited a leaf -like structure over the scan rates ranging from 5 to 200mV/s and the potential window set between -0.1 to 0.6 V, indicating the combined effects of electrical double-layer capacitance (EDLC) and slight pseudocapacitive contributions, as well as intrinsic resistance and ion diffusion limitations within the porous electrode[1,2]. The GCD curves (Figure 6b) exhibit a nearly symmetric triangular shape, indicating good capacitive behavior and reversibility of the electrode material. However, a relatively slower charging profile is observed, which may be attributed to ion diffusion limitations and restricted accessibility of electrolyte ions within the porous structure. This behavior is likely influenced by pore size distribution and internal resistance of the electrode material. The electrode delivered a specific capacitance of 333.8 F g ^{1}, at a current density of 1 A g ^{1}. This value is comparable to previously reported biomass-derived activated carbons, such as peanut shell-derived carbon, date seeds-derived carbon, camellia seeds-derived carbon, etc.

Electrochemical impedance spectroscopy (EIS) was performed to evaluate the resistive and capacitive behavior of the electrode (Figure 6c). The Nyquist plot shows a small semicircle in the high-frequency region followed by an inclined line in the low-frequency region. The intercept on the real axis represents the solution resistance (Rs), which was found to be ~3.5 Ω, indicating moderate internal resistance. The small diameter of the semicircle suggests low charge transfer resistance (*Rct)*, while the inclined line corresponds to Warburg impedance associated with ion diffusion in the porous structure. The deviation from an ideal vertical line indicates some diffusion limitation, which may be attributed to pore structure and the relatively low activation temperature (700°C).

Comparison of KOH-activated biomass- derived carbon electrodes

The electrochemical performance of *Mucuna monosperma* seed-derived activated carbon compares favorably with other biomass-derived carbon materials impregnated with KOH, reported for supercapacitor applications. For instance, activated carbon derived from peanut shells has been reported to exhibit a specific capacitance of approximately 224.3 Fg^{-1} in a three-electrode system, and orange peel- derived carbon has been reported with a specific capacitance of 460 Fg^{-1} in aqueous KOH electrolyte. Similarly, Coconut shell-derived AC showed 386-425 Fg^{-1} with moderate energy and power density values. The comparable performance achieved in the present work, combined with the use of an underutilized biomass precursor, highlights the potential of *Mucuna monosperma* seeds as a sustainable and low-cost carbon source.

Conclusions

Activated carbon was successfully synthesized from

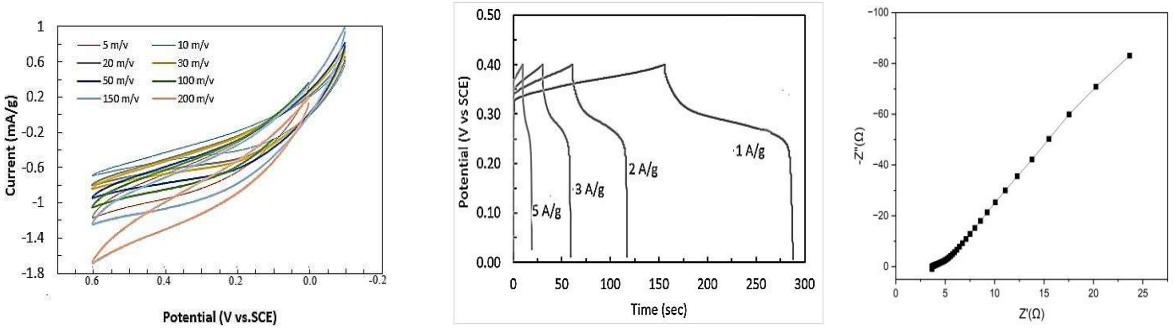

Figure 6: Electrochemical performance of BSC_700 electrode; a) CV curve (left) b) GCD curve (centre) c) EIS plot (rig).

Table 1: Specific capacitance of BSC_700 at different current densities.

Current density (A/g)	Discharge time (s)	Sp. capacitance (F/g)
1	133.5	333.8
2	58.0	290
3	26.2	196.5
5	8.1	101.3

Mucuna monosperma seed biomass via chemical activation (KOH) at 700 °C, demonstrating the effective utilization of an underexplored biomass precursor. The prepared carbon exhibited well-developed porosity, as evidenced by an iodine number of 803.7±35.43 mgg^{-1}, methylene blue adsorption capacity of 674.69±0.76 mg g^{-1}, and a specific surface area of 1360 m^2g^{-1} estimated by Langmuir adsorption isotherm. Boehm titration confirmed a predominantly amorphous carbon framework with favorable surface functional groups and a near-neutral *pHpzc* value of approximately 7.0, supporting effective electrolyte interaction under alkaline conditions. Electrochemical evaluation in 6 M KOH electrolyte revealed electric double-layer capacitive behavior, delivering a good specific capacitance of 333.8 Fg^{-1} at 1 Ag^{-1}, along with low internal resistance. These results demonstrate that *Mucuna monosperma* seed-derived activated carbon is a promising, low-cost, and environmentally friendly electrode material for supercapacitor applications.

Table 2: Comparison of KOH- activated Biomass- Derived Carbons with the Present Work.

Biomass precursor	Specific Capacitance (F/g)	Current density (A/g)	Specific surface area (m^2/g)
Orange peel[18]	460	–	
Peanut Shell[19]	224.3	1.0	2547
Camellia Seeds[20]	305	0.5	1219
Lotus seedpods[21]	169.7	1.0	1369.7
Tea leaves[22]	131.95	0.5	
Horsegram[23]	396	1.0	2037
Baldhyangra seeds (This study)	333.8	1.0	1360

Data Availability Statement

The data used in this study are available from the corresponding author upon reasonable request.

Acknowledgement

The University Grants Commission, Nepal, supported this research through the Collaborative Research Grant (CRG-79/80-S&T-01). The authors thank Prof. Dr Lok Kumar Shrestha and Miss Sabina Shahi, NIMS, MANA, Japan, for recording the FTIR spectra and NAST Nepal for XRD analysis.

References

1. Conway, B. E. 1999. Electrochemical Supercapacitors: Scientific Fundamentals and Technological Applications. First edition, Springer, Boston, MA.
   Doi: https://doi.org/10.1007/978-1-4757-3058-6_2
2. Simon, P. and Gogotsi, Y. 2008. Materials for electrochemical capacitors. *Nature Materials*. **7** (11): 845–854.
   Doi: https://doi.org/10.1038/nmat2297
3. Olabi, A. G., Abbas, Q., Makky, A. A. and Abdelkareem, M. A. 2022. Supercapacitors as next generation energy storage devices: properties and applications. *Energy*. **248**: 123617.
   Doi: https://doi.org/10.1016/j.energy.2022.123617
4. Lemine, A. S., Zagho, M. M., Altahtamouni, T. M. and Bensalah, N.

2018. Graphene a promising electrode material for supercapacitors – a review. *International Journal of Energy Research.* **42** (14): 4284–4300.
Doi: https://doi.org/10.1002/er.4170

5. Wang, F., et al. 2017. Latest advances in supercapacitors: from new electrode materials to novel device designs. *Chemical Society Reviews*. **46** (22): 6816–6854.
Doi: https://doi.org/10.1039/c7cs00205j
6. Wang, Q., Yan, J. and Fan, Z. 2015. Carbon materials for high volumetric performance supercapacitors s: design, progress, challenges and opportunities. *Energy & Environmental Science*. **9** (3): 729–762.
Doi: https://doi.org/10.1039/c5ee03109e
7. Borenstein, A., et al. 2017. Carbon-based composite materials for supercapacitor electrodes: a review. *Journal of Materials Chemistry A*. **5** (25): 12653–12672.
Doi: https://doi.org/10.1039/c7ta00863e
8. Wang, Y., et al. 2020. Recent progress in carbon-based materials for supercapacitor electrodes: a review. *Journal of Materials Science*. **56** (1): 173–200.
Doi: https://doi.org/10.1007/s10853-020-05157-6
9. Gu, W. and Yushin, G. 2013. Review of nanostructured carbon materials for electrochemical capacitor applications: advantages and limitations of activated carbon, carbide-derived carbon, zeolite-templated carbon, carbon aerogels, carbon nanotubes, onion-like carbon, and graphene. *Wiley Interdisciplinary Reviews: Energy and Environment*. **3** (5): 424–473.
Doi: https://doi.org/10.1002/wene.102
10. Zhang, L. L., Gu, Y. and Zhao, X. S. 2013. Advanced porous carbon electrodes. *Journal of Materials Chemistry A*. **1** (33): 9395–9405.
Doi: https://doi.org/10.1039/c3ta11114h
11. Zhang, S., et al. 2022. Understanding synthesis–structure–performance correlations of nanoarchitectured activated carbons for electrochemical applications and carbon capture. *Advanced Functional Materials*. **32** (40).
Doi: https://doi.org/10.1002/adfm.202204714
12. Gupta, N., et al. 2022. Biomass conversion of agricultural waste residues for different applications: a comprehensive review. *Environmental Science and Pollution Research*. **29** (49): 73622–73647.
Doi: https://doi.org/10.1007/s11356-022-22802-6
13. Tripathi, N., Hills, C. D., Singh, R. S. and Atkinson, C. J. 2019. Biomass waste utilisation in low-carbon products: harnessing a major potential resource. *Npj Climate and Atmospheric Science*. **2** (1).
Doi: https://doi.org/10.1038/s41612-019-0093-5
14. Williams, N.E., Oba, O. A. and Aydinlik, N. P. 2022. Modificationproduction, and methods of KOH-Activated Carbon. *ChemBioEng Reviews*. **9** (2): 164–189.
Doi: https://doi.org/10.1002/cben.202100030
15. Wang, J. and Kaskel, S. 2012. KOH activation of carbon-based materials for energy storage. *Journal of Materials Chemistry*. **22** (45): 23710–23725.
Doi: https://doi.org/10.1039/c2jm34066f
16. Duraisamy, N., K, S. K., Dhandapani, E. and Kandiah, K. 2025. A review on biomass-derived activated carbon for next-generation supercapacitors: cutting-edge advances and future prospects. *Energy & Fuels*. **39** (5): 2306–2347.
Doi: https://doi.org/10.1021/acs.energyfuels.4c03842
17. Boehm, H. 1994. Some aspects of the surface chemistry of carbon blacks and other carbons. *Carbon*. **32** (5): 759–769.
Doi: https://doi.org/10.1016/0008-6223(94)90031-0
18. Saini, S., Chand, P. and Joshi, A. 2021. Biomass-derived carbon for supercapacitor applications: review. *Journal of Energy Storage*. **39**: 102646.
Doi: https://doi.org/10.1016/j.est.2021.102646
19. Sylla, N.F., et al. 2019. Effect of porosity-enhancing agents on the electrochemical performance of high-energy ultracapacitor electrodes derived from peanut shell waste. *Scientific Reports*. **9**: 13673.
Doi: https://doi.org/10.1038/s41598-019-50189-x
20. Yang, J., et al. 2024. Activated Carbon Derived from the Agricultural Waste Camellia Seed Shell for High-Performance Supercapacitors. *ACS Applied Energy Materials*. **7** (2): 469–478.
Doi: https://doi.org/10.1021/acsaem.3c02391
21. Boonraksa, N., Swatsitang, E. & Wongsaprom, K. 2024. KOH-activated lotus seedpods carbon. *Materials Science and Engineering B*. **301**: 117151.
Doi: https://doi.org/10.1016/j.mseb.2023.117151
22. Thirumal, V., et al. 2021. Characterization of activated biomass carbon from tea leaf for supercapacitor applications. *Chemosphere*. **291**(pt 2): 132931.
Doi: https://doi.org/10.1016/j.chemosphere.2021.132931
23. Adhikari M.P, Shahi S., Ma. R., Hill J. P.,Ariga K., and Shrestha L. K., 2025. Ultrahigh surface area self-nitrogen-doped nanoporous carbon materials from *Macrotyloma uniflorum* (Horse gram) seed for high-performance supercapacitor applications. *J. Power Sources*. **631**: 3236239.
Doi: https://doi.org/10.1016/j.jpowsour.2025.236239